Bioorg. Med. Chem. 113 (2024) 117937

Contents lists available at ScienceDirect

Bioorganic & Medicinal Chemistry

journal homepage: www.elsevier.com/locate/bmc

Rational design, synthesis, and biophysical characterization of a peptidic MDM2-MDM4 interaction inhibitor

Marco Ballarotto [a,1], Elisa Bianconi [a], Sonia Valentini [b,c], Andrea Temperini [a,*], Fabiola Moretti [c], Antonio Macchiarulo [a,*]

[a] Dipartimento di Scienze Farmaceutiche, Università degli Studi di Perugia, Via del Liceo, 1, 06123 Perugia, Italy
[b] PhD program in Sciences of Nutrition, Metabolism, Ageing and Gender Medicine, Catholic University of Rome, Roma, Italy
[c] Institute of Biochemistry and Cell Biology, National Research Council (CNR), Via E. Ramarini, 32, 00015 Monterotondo Scalo, Rome, Italy

ARTICLE INFO

Keywords:
Cancer
MDM2
MDM4
MDMX
P53
Biophysical techniques
Molecular modelling

ABSTRACT

In recent years, the restoration of p53 physiological functions has become an attractive therapeutic approach to develop novel and efficacious cancer therapies. Among other mechanisms, the oncosuppressor protein p53 is functionally regulated by MDM2 through its E3 ligase function. MDM2 promotes p53 ubiquitination and degradation following homodimerization or heterodimerization with MDM4. Recently, we discovered Pep3 (**1**, Pellegrino *et al.*, 2015), a novel peptidic inhibitor of MDM2 dimerization able to restore p53 oncosuppressive functions both *in vitro* and *in vivo*. In this work, we were able to identify the key interactions between peptide **1** and MDM2 RING domain and to design peptide **2**, a truncated version of **1** that is still able to bind MDM2. Integrating both computational and biophysical techniques, we show that peptide **2** maintains the conserved peptide **1**-MDM2 interactions and is still able to bind to full-length MDM2.

1. Introduction

The transcription factor p53 plays a crucial role in the process of carcinogenesis, to such a degree that it has earned itself the nickname 'guardian of the genome'.[1,2] It has key functions in the transcription of numerous genes involved in DNA repair, cell cycle regulation, apoptosis and tumour suppression.[3,4]

Most human tumours show alterations at the level of the p53 pathway, either showing mutations or deletions in the encoding TP53 gene or changes in the functional regulation of wild-type p53.[5,6] Therefore, reinstating the oncosuppressor function of p53 has become an attractive therapeutic strategy for tumour therapy. In this context, the RING E3 ubiquitin ligase MDM2 has an essential role in modulating p53 activity including, among other mechanisms, the regulation of the protein half-life.[7–11] Indeed, MDM2 promotes the ubiquitination and proteasomal degradation of p53 and its presence is essential for embryonic development.[12,13] Recent evidence has shown that the MDM2 regulatory functions are performed through either homodimerization or heterodimerization with its homolog MDM4 (also MDMX), with the heterodimeric form showing greater degree of p53 suppression.[14,15] It is clear then how MDM2 and MDM4 roles as functional p53 modulators have become the targets of substantial medicinal chemistry efforts that culminated in the development of several MDMs-p53 interaction inhibitors (Fig. 1). However, it has been shown that the sole targeting of either of the two MDMs-p53 interactions is not sufficient to achieve long-term and stable suppression of tumour growth, with all compounds' development being halted at the clinical trials stage.

In this context, inhibiting the MDM2-MDM4 heterodimerization has recently become a potential strategy to more effectively restore p53 functions.[16] With this regard, mutagenesis studies have been carried out to investigate hot spots of such interaction[17] as well as design MDM2 mutants that lack MDM2's E3 activity but retain the ability to limit p53's transcriptional activity.[18] Some natural compounds have been found to bind the MDM2-MDMX RING domain and inhibit MDM2-mediated ubiquitination *in vitro*, with induction of apoptosis in various cancer cell lines.[19]. Overall, these studies support the notion that targeting the

Abbreviations: AcOH, Acetic acid; DCM, Dichloromethane; DIPEA, *N*,*N*-diisopropylethylamine; MD, Molecular Dynamics; MDM2, Mouse Double Minute 2 homolog; MDM4, Mouse Double Minute 4 homolog; MeCN, Acetonitrile; MST, MicroScale Thermophoresis; RING, Really Interesting New Gene; RMSD, Root Mean Square Deviation; RMSF, Root Mean Square Fluctuation..

* Corresponding authors.
E-mail addresses: andrea.temperini@unipg.it (A. Temperini), antonio.macchiarulo@unipg.it (A. Macchiarulo).
[1] Present address: Division of Cancer Therapeutics, Centre for Cancer Drug Discovery, The Institute of Cancer Research, London SM2 5NG, United Kingdom.

https://doi.org/10.1016/j.bmc.2024.117937
Received 19 August 2024; Received in revised form 26 September 2024; Accepted 30 September 2024
Available online 2 October 2024

MDM2-MDM4 heterodimerization process could translate into a more advantageous biological activity profile compared to the currently existing approaches.

To this end, in a previous work, we identified Pep3 (**1**) as a potent inhibitor of MDM2/MDM4 interaction.[20] The identified peptide encompassed the last 12 amino acids of the MDM4 RING domain C-terminus (Lys479^{MDM4}-Ala490^{MDM4}), that are responsible for the interaction with the MDM2 RING domain. Peptide **1** binds the MDM2 RING domain and impairs MDM2-MDM4 heterodimerization, showing effective anticancer activity *in vitro* across multiple cell lines. Gratifyingly, it also showed *in vivo* efficacy on murine xenograft models, resulting in significant tumour growth suppression.

In this work, we detail our efforts in the rational design, synthesis, and biophysical characterization of a shortened version of **1**, with the aim of retaining its biological activity and opening a path to the development of MDM2-MDM4 interaction inhibitors with improved pharmacokinetic properties (e.g. metabolic stability and cell permeability) and synthetic accessibility.

2. Materials and methods

2.1. General remarks

All reagents and solvents were purchased from commercial suppliers. Dry CH_2Cl_2 (DCM) was obtained by treatment with anhydrous $CaCl_2$ for 24 h, then refluxing over P_2O_5 for 1 h, and then distilling. It was then stored over activated molecular sieves. DIPEA was distilled from ninhydrin and then from KOH pellets and stored in an amber bottle placed in the dark over KOH pellets. Diethylamine was distilled from KOH pellets. DMF was obtained as anhydrous and peptide grade from commercial suppliers and used as is. All reactions were performed under Argon if not explicitly specified. Thin Layer Chromatography (TLC) was performed on fluorescent dye-coated silica gel 60 supported on aluminum sheets using UV light (254 nm), 0.5% *w/v* $KMnO_4$ aqueous solution (followed by gentle heating), ninhydrin stain (1% *w/v* solution in Acetone/AcOH 98:2 *v/v*) or iodine for visualization. Flash column chromatography was performed on silica gel (40–63 μm), dry-loading the reaction residue on silica (60–200 μm). ^{1}H NMR spectra were recorded at 25 °C at 400 MHz. Chemical shifts (δ) are reported in parts per million (ppm). The NMR spectra were calibrated using the proton signal of residual non-deuterated solvent peak (7.27 ppm for $CHCl_3$ and 2.50 ppm for $(CD_3)_2SO$). The abbreviations used are as follows: s, singlet; brs, broad singlet; d, doublet; dd, doublet of doublets; dt, doublet of triplets; ddd, doublet of doublet of doublets; t, triplet; q, quartet; m, multiplet. High-Resolution Mass Spectroscopy (HRMS) analyses were carried out on Agilent 6560 Ion Mobility Q-TOF LC-MS system instrument. Mass spectra are recorded using positive mode electro spray ionization (ESI).

2.2. Computational details

All computational modelling was performed using the Schrodinger software suite (v2019-4). All structure manipulation and image exporting operations were performed using Schrodinger Maestro module.[21] Starting from the X-ray structure of the MDM2/MDM4 RING domain heterodimer (PDB code: 2VJF), peptide **1**-MDM2 complex was modelled as previously described.[20] The MDM4 C-terminus was cleaved leaving only the last 12 amino acids. The creation of the molecular systems for the molecular dynamics (MD) simulations and the MD simulation themselves were performed by using Desmond (v6.0).[22,23] with the OPLS3e force field, running on NVIDIA GPUs. The modelled complexes were solvated with SPC water molecules and neutralised by the addition of the appropriate amount of Na^+ or Cl^- ions. The simulation length was 100 ns, recording 500 evenly-spaced frames over the simulation time. The Nosé-Hoover chain thermostat[24] and the Martyna-Tobias-Klein barostat[25] methods were used throughout all the simulations as implemented in Desmond. Starting from the same initial system, the simulations were performed in triplicate by changing the seed for the randomised assignment of the starting velocities.

RMSD and RMSF analyses were done using Schrodinger Simulation Interaction Diagram module and exporting the resulting data as csv files. All plots were created with in-house Python scripts. Molecular docking was performed on the MDM2 chain of the MDM2/MDM4 RING domain heterodimer (chain A, PDB code: 2VJF) and a docking grid suitable for peptide docking was centred on the centre of mass of the last 5 MDM4 residues. The designed peptide **2** was then docked using a peptide-specific protocol with Glide v8.7.[26]

2.3. Synthesis *of* peptide 2

Fmoc-Ile-Ala-OtBu: H_2N-Ala-OtBu hydrochloride (0.182 g, 1 mmol), Fmoc-Ile-OH (0.459 g, 1.3 mmol, 1.3 eq.), HOBt hydrate (0.200 g) and

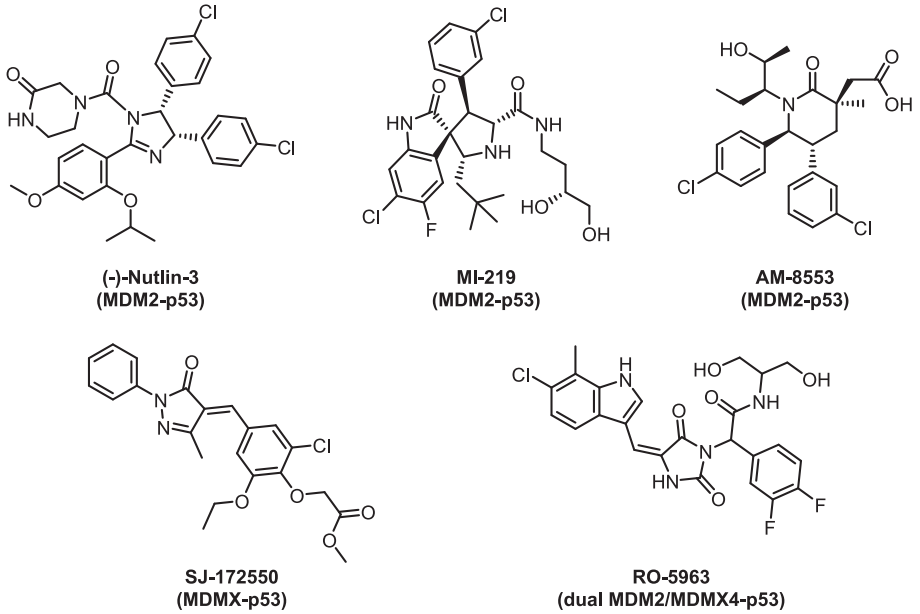

Fig. 1. Known MDM2-p53 and MDM4-p53 interaction inhibitors and their respective mode of action.

DIPEA (0.61 mL, 3.5 mmol, 3.5 eq.) were dissolved in dry DCM. EDC hydrochloride (0.249 g, 1.3 mmol, 1.3 eq.) was added all at once at room temperature, and the reaction mixture was stirred for 24 h. The reaction mixture was then transferred into a separating funnel with EtOAc and washed three times with 5% (*w/v*) aqueous $NaHSO_4$, three times with 5% (*w/v*) aqueous $NaHCO_3$, once with brine and dried over Na_2SO_4. The solvent was removed in vacuo and the residue was purified by dry-loading flash column chromatography on silica gel (eluent: DCM/EtOAc 95:5) to give the protected dipeptide as a white solid (0.359 g, 0.75 mmol, 75%). The spectral data was in agreement with the literature values.[27]

Fmoc-Phe-Ile-Ala-OtBu: Fmoc-Ile-Ala-OtBu (0.360 g, 0.75 mmol) was suspended in a MeCN/DCM mixture (8:1 *v/v*, 9 mL, 0.1 M). Diethylamine (2 mL) was added at room temperature and the reaction was stirred until reaction completion was detected by TLC. The volatiles were removed *in vacuo* and the residue was dissolved in dry DCM (5 mL). To this solution Fmoc-Phe-OH (0.58 g, 1.5 mmol, 2 eq.), HOBt hydrate (0.350 g) and DIPEA (0.33 mL, 1.9 mmol, 2.5 eq.) were added. EDC hydrochloride (0.290 g, 1.5 mmol, 2.0 eq.) was added all at once at room temperature and the reaction mixture was stirred for 16 h. The reaction mixture was then transferred into a separating funnel with EtOAc and washed three times with 5% (*w/v*) aqueous $NaHSO_4$, three times with 5% (*w/v*) aqueous $NaHCO_3$, once with brine and dried over Na_2SO_4. The solvent was removed *in vacuo* and the residue was purified by dry-loading flash column chromatography on silica gel (eluent: DCM/EtOAc 90:10) to give the desired protected tripeptide as a white solid (0.408 g, 0.73 mmol, 98%). ^{1}H NMR (400 MHz, $CDCl_3$) $\delta = 7.76$ (d, $J =$ 7.5 Hz, 2H), 7.53 (*pseudo* t, $J = 6.4$ Hz, 2H), 7.40 (t, $J = 7.5$ Hz, 2H), 7.34–7.13 (m, 7H), 6.46 (brs, 1H), 6.31 (brs, 1H), 5.36 (brs, 1H), 4.54–4.27 (m, 4H), 4.26–4.14 (m, 2H), 3.09 (brs, 2H), 1.90–1.74 (m, 1H), 1.46 (s, 9H), 1.42–1.27 (m, 4H), 1.12–0.97 (m, 1H), 0.85 (t, $J = 6.9$ Hz, 6H). HRMS (ESI-TOF) *m/z*: $[M + H]^+$ calcd. for $C_{37}H_{46}N_3O_6^+$, 628.3386; found 628.3373.

Fmoc-Val-Phe-Ile-Ala-OtBu: Fmoc-Phe-Ile-Ala-OtBu (0.224 g, 0.4 mmol) was dissolved in DMF (4 mL, 0.1 M). Diethylamine (1 mL) was added at room temperature and the reaction was stirred until reaction completion was detected by TLC. The diethylamine was removed *in vacuo* and to the resulting solution was added Fmoc-Val-OH (0.196 g, 0.52 mmol, 1.3 eq.), HOBt hydrate (0.200 g) and DIPEA (0.16 mL, 0.9 mmol, 2.5 eq.). EDC hydrochloride (0.100 g, 0.52 mmol, 1.3 eq.) was added all at once at room temperature and the reaction mixture was stirred for 16 h. The reaction mixture was then transferred into a separating funnel with EtOAc and washed three times with 5% (*w/v*) aqueous $NaHSO_4$, three times with 5% (*w/v*) aqueous $NaHCO_3$, once with brine and dried over Na_2SO_4. The solvent was removed *in vacuo* and the residue was purified by dry-loading flash column chromatography on silica gel (eluent: DCM/EtOAc 80:20) to give the desired protected tetrapeptide as a white solid (0.157 g, 0.23 mmol, 54%).^{1}H NMR (400 MHz, $DMSOd_6$) $\delta = 8.28$ (d, $J = 6.8$ Hz, 1H), 8.02 (d, $J = 8.2$ Hz, 1H), 7.90 (d, $J = 7.7$ Hz, 2H), 7.84 (d, $J = 8.2$ Hz, 2H), 7.73 (t, $J = 6.2$ Hz, 2H), 7.42 (*pseudo* t, $J = 7.3$ Hz, 2H), 7.37–7.27 (m, 3H), 7.25–7.15 (m, 4H), 7.14—7.08 (m, 1H), 4.67–4.57 (m, 1H), 4.36–4.06 (m, 5H), 3.87 (t, $J = 8.2$ Hz, 1H), 2.98 (dd, $J = 14.1$, 4.1 Hz, 1H), 2.78 (dd, $J = 14.1$, 9.6 Hz, 1H), 1.94–1.82 (m, 1H), 1.75–1.62 (m, 1H), 1.50–1.38 (m, 1H), 1.39 (s, 9H), 1.24 (d, $J = 6.9$ Hz, 3H), 1.14–1.02 (m, 1H), 0.85 (d, $J = 6.4$ Hz, 3H), 0.83–0-69 (m, 9H). HRMS (ESI-TOF) *m/z*: $[M + H]^+$ calcd. for $C_{42}H_{55}N_4O_7^+$, 727.4070; found 727.4062.

Fmoc-Lys(Boc)-Val-Phe-Ile-Ala-OtBu: Fmoc-Val-Phe-Ile-Ala-OtBu (0.212 g, 0.29 mmol) was dissolved in DMF (4 mL, 0.075 M). Diethylamine (4 mL) was added at room temperature and the reaction was stirred for 16 h. The diethylamine was removed *in vacuo* and to the resulting solution was added Fmoc-Lys(Boc)–OH (0.164 g, 0.35 mmol, 1.2 eq.) and DIPEA (0.12 mL, 0.64 mmol, 2.2 eq.). COMU (0.150 g, 0.35 mmol, 1.2 eq.) was added all at once at room temperature and the reaction mixture was stirred for 16 h. The reaction mixture was then transferred into a separating funnel with EtOAc and washed three times with 5% (*w/v*) aqueous $NaHSO_4$, three times with 5% (*w/v*) aqueous $NaHCO_3$, twice with brine and dried over Na_2SO_4. The solvent was removed *in vacuo* and the residue was purified by flash column chromatography on silica gel (eluent: DCM/MeOH 96:4) to give the desired protected pentapeptide as a white solid (0.231 g, 0.24 mmol, 83%). HRMS (ESI) *m/z*: [M + Na] + calcd. for $C_{53}H_{74}N_6O_{10}Na^+$, 977.5364; found 977.5438. ^{1}H NMR (400 MHz, $DMSOd_6$) $\delta = 8.27$ (d, $J = 6.7$ Hz, 1H), 8.07 (d, $J = 7.8$ Hz, 1H), 7.88 (d, $J = 7.6$ Hz, 2H), 7.84 (d, $J = 8.9$ Hz, 1H), 7.69 (*pseudo* t, $J = 6.0$ Hz, 2H), 7.64 (d, $J = 10.0$ Hz, 1H), 7.49 (d, $J = 8.3$ Hz, 1H), 7.40 (d, $J = 7.5$ Hz, 2H), 7.30 (*pseudo* t, $J = 7.0$ Hz, 2H), 7.24—7.10 (m, 5H), 6.77 (t, $J = 5.2$ Hz, 1H), 4.63–4.54 (m, 1H), 4.30–4.03 (m, 6H), 4.02–3.92 (m, 1H), 2.98–2.80 (m, 3H), 2.80–2.70 (m, 1H), 1.84–1.81 (m, 1H), 1.73–1.60 (m, 1H), 1.53–1.27 (m, 7H), 1.35 (s, 18H), 1.22 (d, $J = 7.1$ Hz, 3H), 1.12–1.03 (m, 1H), 0.84 (d, $J = 6.8$ Hz, 3H), 0.78 (t, $J = 7.2$ Hz, 3H), 0.76–0.68 (m, 6H). ^{1}HRMS (ESI-TOF) *m/z*: $[M + H]^+$ calcd. for $C_{25}H_{36}NO_3S^+$, 430.2415; found 430.2417.

H_2N-Lys-Val-Phe-Ile-Ala-OH (**2**): Fmoc-Lys(Boc)-Val-Phe-Ile-Ala-OtBu (0.060 g, 0.06 mmol) was dissolved in DCM (1 mL, 0.06 M). Diethylamine (1 mL) was added and the reaction was stirred at room temperature for 16 h. The volatiles were removed *in vacuo* and the residue was purified by flash column chromatography (eluent: gradient from DCM/MeOH 94:6 to 90:10) to give the Boc-protected intermediate as a pale-yellow resin (0.039 g) which was dissolved in DCM (0.5 mL). TFA (peptide grade, 0.5 mL) was added to this mixture at room temperature and the reaction was stirred for 4 h, after which the volatiles were removed *in vacuo*.The residual TFA was removed by repeatedly redissolving the residue in DCM and drying the residue it *in vacuo*. The off-white residue was then triturated with cold (−20 °C) Et_2O, filtered on a Buchner funnel and dried overnight in a vacuum desiccator over $P_2O_5$to give the product as the bis-trifluoroacetate salt as an off-white solid (0.022 g, 0.027 mmol, 52%).HRMS (ESI) *m/z*: $[M + 2H]^{2+}$ calcd. for $C_{29}H_{50}N_6O_6^{2+}$, 289.1895; found 289.19039.

2.4. Synthesis of peptide 3

Fmoc-Lys(Boc)-Phe-OtBu: Fmoc-Lys(Boc)–OH (0.824 g, 1.76 mmol), H_2N-Phe-OtBu hydrochloride (0.500 g, 1.94 mmol, 1.1 eq.), HOBt hydrate (0.400 g) and EDC hydrochloride (0.372 g, 1.94 mmol, 1.3 eq.) were dissolved in dry DCM (20 mL, 0.1 M). DIPEA (1.0 mL, 5.82 mmol, 3 eq.) was added all at once at room temperature and the reaction mixture was stirred for 24 h. The reaction mixture was then transferred into a separating funnel with DCM and washed three times with 0.1 M aqueous HCl, three times with 5% (*w/v*) aqueous $NaHCO_3$, once with brine and dried over Na_2SO_4. The solvent was removed in vacuo and the residue was purified by dry-loading flash column chromatography on silica gel (eluent: DCM/MeOH 97:3) to give the protected dipeptide as a white solid (1.01 g, 1.50 mmol, 85%). The spectral data was in agreement with the literature values.[28]

Fmoc-Ile-Lys(Boc)-Phe-OtBu: Fmoc-Lys(Boc)-Phe-OtBu (0.098 g, 0.15 mmol) was dissolved in DCM (4 mL, 0.04 M). Diethylamine (1 mL) was added at room temperature and the reaction was stirred for 3 h. The volatiles were removed *in vacuo* and the residue was dissolved in dry DMF (3 mL). To this solution Fmoc-Ile-OH (0.103 g, 0.29 mmol, 2 eq.), and DIPEA (0.09 mL, 0.51 mmol, 3.5 eq.) were added. COMU (0.125 g, 0.29 mmol, 2.0 eq.) was added all at once at room temperature and the reaction mixture was stirred for 16 h. The reaction mixture was then transferred into a separating funnel with EtOAc and washed three times with 5% (*w/v*) aqueous $NaHSO_4$, three times with 5% (*w/v*) aqueous $NaHCO_3$, once with brine and dried over Na_2SO_4. The solvent was removed *in vacuo* and the residue was purified by dry-loading flash column chromatography on silica gel (eluent: DCM/MeOH 97:3) to give the protected tripeptide as a white solid (0.092 g, 0.12 mmol, 80%).^{1}H NMR (400 MHz, $CDCl_3$) $\delta = 7.78$ (d, $J = 7.5$ Hz, 2H), 7.60 (d, $J = 7.3$ Hz, 2H), 7.41 (*pseudo* t, $J = 7.4$ Hz, 2H), 7.32 (*pseudo* t, $J = 7.6$ Hz, 2H), 7.30—7.20 (m, 3H), 7.14 (d, $J = 6.9$ Hz, 2H), 6.49 (d, $J = 7.3$ Hz, 1H), 6.41 (d, $J = 7.4$ Hz, 1H), 5.47 (d, $J = 8.0$ Hz, 1H), 4.78–4.64 (m, 2H),

4.49–4.30 (m, 3H), 4.23 (t, J = 6.9 Hz, 1H), 3.33–2.96 (m, 4H), 1.93–1.77 (m, 2H), 1.66–1.37 (m, 4H), 1.43 (s, 9H), 1.41 (s, 9H), 1.35–1.22 (m, 3H), 1.20–1.08 (m, 1H), 0.97–0.81 (m, 6H).

Fmoc-Ala-Ile-Lys(Boc)-Phe-OtBu: Fmoc-Ile-Lys(Boc)-Phe-OtBu (0.092 g, 0.12 mmol) was dissolved in MeCN (2 mL, 0.06 M). Diethylamine (0.5 mL) was added at room temperature and the reaction was stirred for 2 h. The volatiles were removed *in vacuo* and the residue was dissolved in dry DCM (5 mL). To this solution Fmoc-Ala-OH (0.074 g, 0.24 mmol, 2 eq.), HOBt hydrate (0.050 g), and DIPEA (0.09 mL, 0.53 mmol, 4.5 eq.) were added. EDC hydrochloride (0.045 g, 0.24 mmol, 2.0 eq.) was added all at once at room temperature and the reaction mixture was stirred for 16 h. The reaction mixture was then transferred into a separating funnel with EtOAc and washed twice with 5% (*w/v*) aqueous $NaHSO_4$, three times with 5% (*w/v*) aqueous $NaHCO_3$, once with brine and dried over Na_2SO_4. The solvent was removed *in vacuo* and the residue was purified by dry-loading flash column chromatography on silica gel (eluent: DCM/MeOH 97:3) to give the protected tetrapeptide as a white solid (0.076 g, 0.09 mmol, 76%). ^{1}H NMR (400 MHz, $DMSOd_6$) δ = 8.19 (d, J = 6.3 Hz, 1H), 7.88 (d, J = 6.9 Hz, 2H), 7.77 (d, J = 7.9 Hz, 1H), 7.75–7.66 (m, 2H), 7.57 (d, J = 7.4 Hz, 1H), 7.41 (t, J = 6.9 Hz, 2H), 7.33 (d, J = 7.0 Hz, 2H), 7.29—7.12 (m, 5H), 6.75 (brs, 1H), 4.40–4.06 (m, 7H), 3.00–2.78 (m, 4H), 1.75–1.64 (m, 1H), 1.64–1.53 (m, 1H), 1.53–1.10 (m, 10*H*), 1.36 (s, 9H), 1.29 (s, 9H), 1.09–0.96 (m, 1H), 0.86–0.70 (m, 6H).

H_2N-Val-Ala-Ile-Lys-Phe-OH (**3**): Fmoc-Ala-Ile-Lys(Boc)-Phe-OtBu (0.094 g, 0.11 mmol) was dissolved in MeCN (2 mL, 0.05 M). Diethylamine (0.5 mL) was added at room temperature and the reaction was stirred for 16 h. The volatiles were removed *in vacuo* and the residue was dissolved in dry DCM (5 mL). To this solution Boc-Val-OH (0.048 g, 0.22 mmol, 2 eq.) and DIPEA (0.07 mL, 0.4 mmol, 3.5 eq.) were added. COMU (0.094 g, 0.22 mmol, 2.0 eq.) was added all at once at room temperature and the reaction mixture was stirred for 16 h. The reaction mixture was then transferred into a separating funnel with EtOAc and washed twice with 5% (*w/v*) aqueous $NaHSO_4$, three times with 5% (*w/v*) aqueous $NaHCO_3$, once with brine and dried over Na_2SO_4. The solvent was removed *in vacuo* and the residue was purified by dry-loading flash column chromatography on silica gel (eluent: DCM/MeOH 97:3) to give the expected fully protected pentapeptide as a white solid (0.055 g, 0.07 mmol, 60%). Unfortunately, it was not possible to prepare an adequate sample for the 1H NMR analysis as the substance is practically insoluble in the classic solvents used, and in some cases a gel is formed. Then, we moved on to the next deprotection step by adding anisole (0.2 mL) and dry DCM (3 mL, 0.05 M) to the above isolated product.TFA (peptide grade, 1 mL) was added dropwise at 0 °C and the mixture was stirred at the same temperature for 4 h, after which the volatiles were removed *in vacuo*. The residual TFA was removed by repeatedly redissolving the residue in DCM and drying the solution *in vacuo*. The off-white residue was then triturated with cold (−20 °C) pentane, until no residual anisole could be identified in the supernatant. The product was obtained as the bis-trifluoroacetate salt as an off-white solid (0.037 g, 0.05 mmol, 73%). HRMS (ESI) *m/z*: $[M + 2H]^{2+}$ calcd. for $C_{29}H_{50}N_6O_6^{2+}$, 289.1895; found 289.1891.

2.5. Production of recombinant human MDM2

Full-length MDM2 was produced in bacteria (BL21 cells) as inducible conjugated GST-MDM2. The protein was isolated by salt precipitation with increasing concentrations of ammonium sulfate (AmSO4) and purified by glutathione agarose resin. In the end, the GST was removed by thrombin (Sigma-Merck) cleavage, and recombinant MDM2 was concentrated with Amicon® Ultra 4 mL (30MWCO). The purification and quantification were performed using Coomassie gel.

2.6. MST binding assays

Recombinant human MDM2 was fluorescently labelled with RED dye NT-650 using the 2nd generation Monolith Protein Labelling Kit RED-NHS (NanoTemper Technologies, Munich, Germany). According to the recommended protocol, 1:6 protein:dye ratio was used. Specifically, 100 μL of 10 μM MDM2 was prepared and mixed with 100 μL of 60 μM RED dye in HEPES-T Buffer (20 mM HEPES, 150 mM NaCl, pH 7.4, 0.05% Tween20). The labelling solution was incubated for 30 min at room temperature in dark conditions. The unreacted fluorophore was removed using a HEPES-*T*-equilibrated size-exclusion chromatography column, which is included in the labelling kit. Protein and dye concentrations were determined by Absorption Spectroscopy using Thermo Scientific™ NanoDrop™ One spectrophotometer (Thermo Fisher Scientific Inc., Waltham Massachusetts, USA) through the equations (1) and (2), where $\varepsilon_{protein}$ = 344235 M^{-1} cm^{-1} at 280 nm (calculated with the ProtParam webserver,[29] Swiss Institute of Bioinformatics), $\varepsilon_{RED\ dye}$ = 195000 M^{-1} cm^{-1} at 650 nm (supplied by the kit vendor), correction factor (cf) = 0.04 (supplied by the kit vendor) and l was the optical path length of the instrument.

$$[protein] = \frac{A_{280} - (A_{650} \times cf)}{\varepsilon_{protein} \times 1} \quad (1)$$

$$[dye] = \frac{A_{650}}{\varepsilon_{REDdye} \times 1} \quad (2)$$

Therefore, the Degree of Labelling (DoL) were calculated using the equation (3), yielding 0.32.

$$DoL = \frac{[dye]}{[protein]} \quad (3)$$

The ligand binding experiments were performed in HEPES-T buffer with the addition of $ZnCl_2$ and DMSO to reach final concentrations of 100 μM and 2%, respectively. All the peptides were tested by titrating with serial dilutions starting from 1 mM as the highest concentration against 50 nM of labelled protein. After 60 min of incubation at room temperature in dark conditions, the samples were briefly centrifuged at 10000 rpm, loaded into standard capillary tubes (MO − K022; NanoTemper Technologies, Munich, Germany) and inserted into the Monolith NT.115 instrument (NanoTemper Technologies, Munich, Germany). MST signals were recorded for each capillary at high laser power and 60% LED power. The raw data were processed by *MO.Affinity Analysis v2.3*, in *Manual mode* (*19/20 s hot regions*). Every experiment was performed in triplicate and the K_d results were reported as mean value with confidence interval (±) that defines the range where the K_d falls with a 68% of certainty.

The SDS denaturation test, or SD-Test, was performed for the long peptide experiments. For this purpose, the remainder of tubes 1 to 3 and 14 to 16 prepared in the original binding assay were centrifuged for 10 min at 12560 rpm. Then, 10 μL of each sample was removed and mixed with 10 μL of SD-mix (4% SDS, 40 mM DTT). After incubation for 5 min at 95 °C to denature the protein, the samples were loaded into standard capillaries and the fluorescence emission was analysed using the Monolith NT.115 instrument.

3. Results and discussion

3.1. Computational evaluation of MDM2-MDM4 RING domain interaction

Starting from the X-ray structure of the MDM2/MDM4 RING domain heterodimer (PDB code: 2VJF), the **1**-MDM2 complex was modelled as described.[20] The MDM4 C-terminus was cleaved leaving only the last 12 amino acids that comprise the structure of **1** ($Lys479^{MDM4}$-$Ala490^{MDM4}$). The modelled complex was then solvated with water molecules and neutralised by the addition of the appropriate amount of Cl ions. The so obtained system was used to perform molecular dynamics (MD) simulations (100 ns, performed in triplicate) to understand the nature and

stability of the key interactions between **1** and MDM2 RING domain. The analysis of the RMSD (Root Mean Square Deviation, Fig. 2A) of the peptide heavy atoms over time, highlighted a significant conformational change in the first 20 ns of simulation. The initial high RMSD absolute value can be ascribed to the choice of the starting conformation, derived from a crystal structure of the full-length MDM4 RING domain. Nonetheless, peptide **1** showed relatively high instability even after the system reached equilibrium in the later stages of simulation, as evidenced by the high standard deviation of the RMSD across the replicas. Prompted by this, the RMSF (Root Mean Square Fluctuation, Fig. 2B) values of the ligand atoms were calculated to gain some insight into the reasons for this binding instability. The RMSF value describes the average RMSD of a specific atom over the duration of the MD simulation and it can help identify what molecule fragments do not take part in a stable interaction. A large RMSF value was observed in the *N*-terminal six residues of **1** aminoacidic sequence (Lys479-Val484). This result suggests that these residues are not stably interacting with MDM2 and that their contribution to the binding of **1** to MDM2 is limited. A slightly large RMSF value was also observed for Lys486, but upon deeper investigation, it was highlighted that the solvent-exposed sidechain is responsible for the apparent instability of the residue (Fig. 2B, inset). Based on these results, we formulated the hypothesis that the last 5 amino acids (Lys486-Ala490) of **1** were responsible for its binding to MDM2 and that a truncated version of **1** comprising those residues would still maintain its ability to inhibit MDM2 dimerization.

To validate our hypothesis *via* computational methods, molecular docking was performed on the MDM2chain of the MDM2/MDM4 RING domain heterodimer (chain A, PDB code: 2VJF) to assess the binding mode of the newly designed peptide **2** (Lys486-Ala490). Differently from the original peptide **1**, where the C-terminus was capped as a primary amide, the terminal Ala residue of **2** was designed as a free carboxylic acid, with the goal of interacting with a salt bridge with the nearby Lys446^{MDM2} for a further point of interaction. The docking performance was evaluated using the RMSD between the backbones of the docked peptide and the crystallised MDM4C-terminus fragment. Satisfyingly, 60% (12/20) of the predicted poses correctly reproduced the crystalised conformation with an RMSD lower than 2.0 Å (Fig. 3A). In particular, the backbone of **2** was positioned close to a MDM2 β-sheet to form a network of hydrogen bonds with MDM2 residues Lys454-Leu458. As expected, we observed a salt bridge between the negatively charged **2** C-terminus and the cationic Lys446 side chain.

Finally, we performed MD simulations starting from the best scoring-docking pose that was consistent with the co-crystallised binding mode. It was observed that the polar interactions initially highlighted by docking were maintained over the simulation time (Fig. 3B). Indeed, the complex canonical network of hydrogen bonds with one of MDM2 RING domain β-sheets was mainly intact over the simulation time, together with the salt bridge between the C-terminus and Lys446^{MDM2}. Moreover, a key interaction of Ile489 sidechain with an hydrophobic pocket in MDM2 structure lined by Leu458^{MDM2}, Pro431^{MDM2}, and the backbone of Asn433^{MDM2} was highlighted (Fig. 3C), confirming the observed experimental results that showed the importance of this residue for peptide **1** binding.[20]

3.2. Synthesis

With strong support from the performed computational modelling, we decided to synthesise peptide **2** (sequence: H_2N-KVFIA-CO_2H)[30] and characterise its interaction with MDM2 in a biophysical assay. Moreover, we included in the biophysical characterization another peptide with a scrambled sequence (**3**, sequence: H_2N-VAIKF-CO_2H) to validate the key interactions highlighted during the modelling and to evaluate the sequence-specificity of the binding to MDM2. Indeed, if the proposed binding mode of peptide **1** is conserved, the substitution of the Ile residue in peptide **2** should completely abolish the binding affinity of the peptide, as it was already observed for the original peptide **1.**[20]

The synthesis of both peptides was performed in solution using a Boc/Fmoc synthetic strategy, using standard amide coupling protocols (see Materials and Methods for details). After the final deprotection, the pure peptides **2** and **3** were obtained as trifluoroacetate salts on a decamilligram scale,with excellent purity by HPLC/MS analysis (14% and 23% overall yields, respectively).

3.3. MicroScale Thermophoresis Binding Assays

The thermophoresis phenomenon describes the directed motion of a macromolecule in a temperature gradient, depending on its size, conformation, charge and hydration shell. For this reason, after a binding event to the target macromolecule, at least one of these parameters is altered and then, thermophoresis of the complex and macromolecule alone is different.[31] In a MicroScale Thermophoresis (MST) experiment, sixteen capillary tubes are prepared, where the fluorescently labelled protein (target) is present at constant concentration and it is titrated by increasing concentrations of the unlabelled ligand.

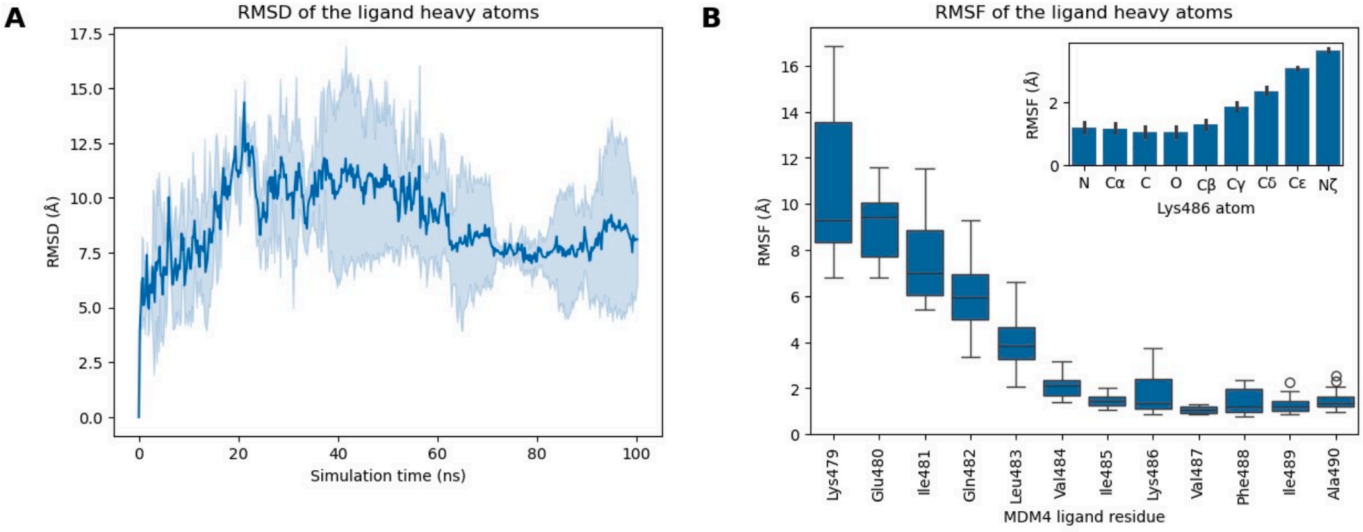

Fig. 2. Analysis of the MD simulations on the peptide 1-MDM2 complex (100 ns, triplicate). (A) The RMSD data is reported as the average (dark blue line) and standard deviation (light blue area). (B) The RMSF data is reported by grouping the ligand atoms by their residue name and number in the MDM4 sequence. Inset: atom-by-atom RMSF contribution of Lys486, shown as mean (bar plot) and standard deviation (error bars).

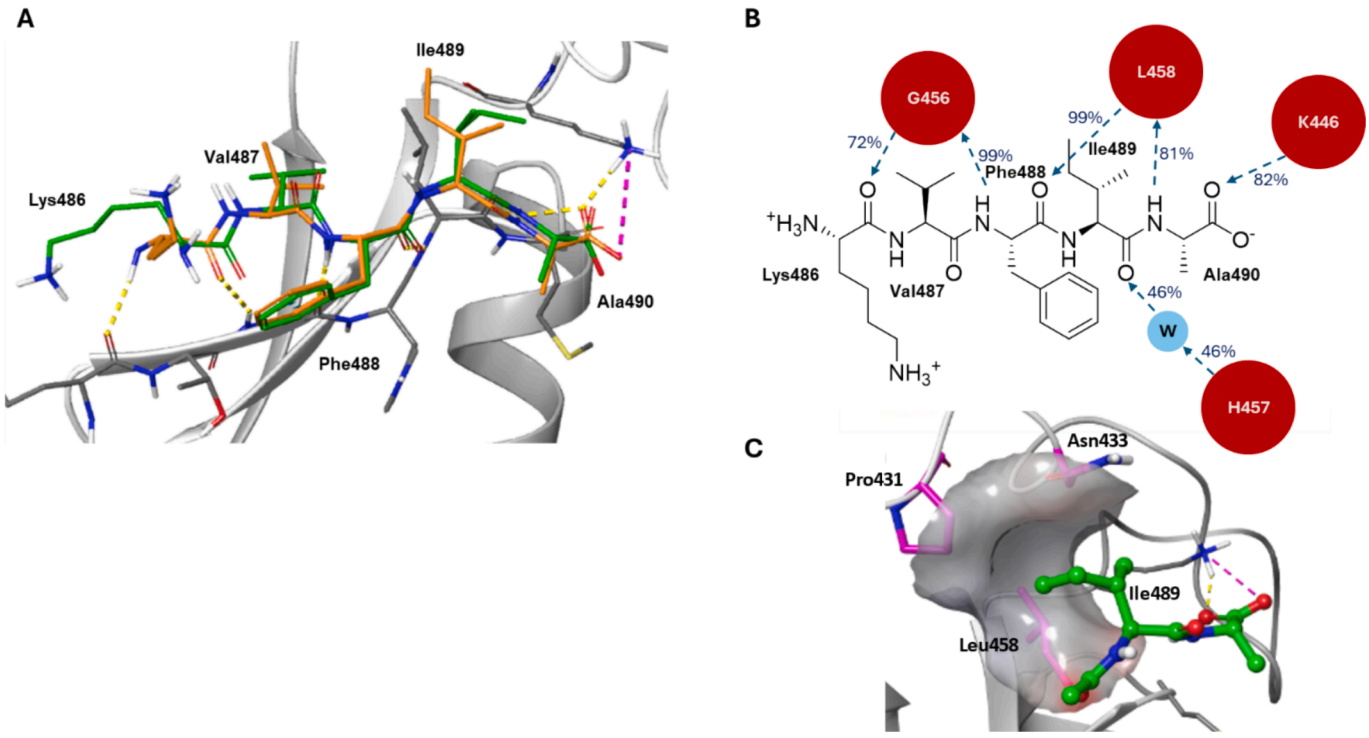

Fig. 3. (A) Putative binding mode of peptide2 to MDM2 RING domain. The docked peptide has been represented as green sticks, the crystalised MDM4 fragment as orange sticks and MDM2 as white ribbons. H-bonds and the ionic interaction are shown in yellow and magenta dashed lines. (B) Interaction occupancy during MD simulation of peptide 2-MDM2 complex. (C) Snapshot of Ile489 side chain interactions during the simulation. Interacting MDM2 residues are highlighted in magenta. ESP surface has been calculated for residues surrounding Ile489.

Within the instrument, an infrared laser induces the temperature gradient in the samples and the protein/ligand complex migrates along it, producing a modulation of the fluorescence signal that can be monitored in real-time. This variation is used to generate a binding curve as a function of ligand concentration and to derive the dissociation constant (K_d).[32]

Peptides **2** and **3** were tested in an MST assay against recombinant fluorescently labelled full-length human MDM2 protein. Pleasingly, a significant dose-dependent variation of the thermophoretic signal was observed for the protein in the presence of increasing concentrations of peptide **2** ($K_d = 19.2 \pm 5.4$ μM, Fig. 4), indicating a clear binding event to MDM2. As predicted, the experiment with peptide **3** did not result in a detectable binding event ($K_d > 1000$ μM, Fig. 4), confirming the direct and specific interaction between peptide **2** and the full-length protein.

In addition, we also tested in the same MST assay the original peptide **1** (sequence: Ac-KEIQLVIKVFIA-NH_2) and a control peptide **4** (sequence: Ac-KEIQLVIFVIKA-NH_2). The control peptide was obtained by swapping Ile489 and Lys486 in the MDM4 sequence, since peptide analogues

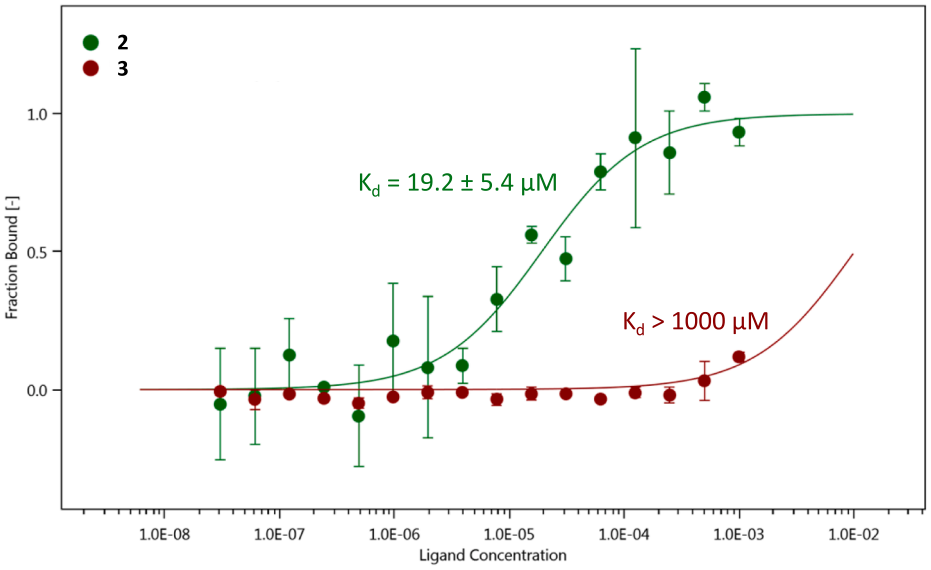

Fig. 4. Binding curve obtained for peptides 2 (green) and 3(red) against full-length recombinant human MDM2. The fraction bound is plotted against ligand concentration, data indicated as mean ± standard deviation (n = 3).

missing the key MDM4 residue Ile489 have been previously shown not to be able to modulate p53 ubiquitination *in vitro*.[20] Unfortunately, the tested full-length peptides induced a ligand-dependent initial fluorescence variation of the samples (Fig. S1, A and B) that could not be ascribed to a specific ligand–protein interaction but to protein precipitation or aggregation.

4. Conclusion

The publicly available MDM2-MDM4 crystal structures were used to generate a binding model for peptide **1**, comprising the last 12 residues of MDM4 C-terminus sequence, that is able to disrupt MDM2 dimerization processes and restore p53 oncosuppressive functions both *in vitro* and *in vivo*.[20] MD simulations performed in triplicate have highlighted several conserved polar and hydrophobic interactions between peptide **1** and MDM2 RING domain, that were then used to design a shorter version of the peptide. The putative binding mode of the designed peptide **2** was analysed both by molecular docking and MD simulations, highlighting the same set of interactions that were observed in the original peptide **1**. The designed peptide **2** was then synthesised through an in-solution synthetic protocol, obtaining the final peptide in decamilligram scale. Peptide **2** was then subjected to an MST binding assay, confirming its binding affinity for recombinant full-length MDM2. Unfortunately, we were not able to assess the binding affinity of the original peptide **1** due to its unspecific interaction with the protein, hindering a direct comparison of binding affinities and competitive experiments. Nonetheless, further studies will be directed at the complete biological characterization of peptide **2**, with the goal of advancing our understanding of MDM2 biology and developing more advanced inhibitors of MDM2-MDM4 interaction for therapeutic purposes. Another approach similar to the one discussed in this paper has been recently published by Merlino *et al.* [33], further validating our experimental and computational results.

Funding

This work was supported by the Università degli Studi di Perugia within the financing program "Fondo Ricerca di Base, 2020", by "Consorzio Interuniversitario Nazionale Metodologie e Processi Innovativi di Sintesi" (C.I.N.M.P.I.S.; project title "Studio e sintesi di oligopeptidi per ostacolare l'interazione tra le proteine MDM2 e MDMX"), and by the Italian Association for Cancer Research Grant, AIRC IG 21814 to F.M.

CRediT authorship contribution statement

Marco Ballarotto: Writing – review & editing, Writing – original draft, Visualization, Methodology, Investigation, Formal analysis. **Elisa Bianconi:** Writing – review & editing, Writing – original draft, Visualization, Methodology, Investigation, Formal analysis. **Sonia Valentini:** Writing – original draft, Methodology, Investigation. **Andrea Temperini:** Writing – review & editing, Supervision, Resources, Project administration, Investigation, Funding acquisition. **Fabiola Moretti:** Writing – review & editing, Supervision, Resources, Project administration, Funding acquisition, Conceptualization. **Antonio Macchiarulo:** Writing – review & editing, Supervision, Resources, Project administration, Funding acquisition, Conceptualization.

Declaration of competing interest

The authors declare the following financial interests/personal relationships which may be considered as potential competing interests: Antonio Macchiarulo reports financial support was provided by Consorzio Interuniversitario Nazionale Metodologie e Processi Innovativi di Sintesi (C.I.N.M.P.I.S). Fabiola Moretti reports financial support was provided by the Italian Association for Cancer Research Grant (AIRC IG 21814). Andrea Temperini reports financial support was provided by Consorzio Interuniversitario Nazionale Metodologie e Processi Innovativi di Sintesi (C.I.N.M.P.I.S). Antonio Macchiarulo has patent #IT102023000015816 pending to CNR, Via del Fosso di Fiorano 64, 00143 Roma. Fabiola Moretti has patent #IT102023000015816 pending to CNR, Via del Fosso di Fiorano 64, 00143 Roma. Andrea Temperini has patent #IT102023000015816 pending to CNR, Via del Fosso di Fiorano 64, 00143 Roma. Marco Ballarotto has patent #IT102023000015816 pending to CNR, Via del Fosso di Fiorano 64, 00143 Roma. Sonia Valentini has patent #IT102023000015816 pending to CNR, Via del Fosso di Fiorano 64, 00143 Roma. If there are other authors, they declare that they have no known competing financial interests or personal relationships that could have appeared to influence the work reported in this paper.

Data availability

Data will be made available on request.

Acknowledgements

We thank Dr. Fulvio Saccoccia for useful discussion.

Appendix A. Supplementary data

Supplementary data to this article can be found online at https://doi.org/10.1016/j.bmc.2024.117937.

References

1. Lane DP. p53, guardian of the genome. *Nature*. 1992;358:15–16. https://doi.org/10.1038/358015a0.
2. Levine AJ. p53, the Cellular Gatekeeper for Growth and Division. *Cell*. 1997;88:323–331. https://doi.org/10.1016/S0092-8674(00)81871-1.
3. Wade M, Li YC, Wahl GM. MDM2, MDMX and p53 in oncogenesis and cancer therapy. *Nat Rev Cancer*. 2013;13:83–96. https://doi.org/10.1038/nrc3430.
4. Stiewe T. The p53 family in differentiation and tumorigenesis. *Nat Rev Cancer*. 2007;7:165–167. https://doi.org/10.1038/nrc2072.
5. Olivier M, Hollstein M, Hainaut P. TP53 Mutations in Human Cancers: Origins, Consequences, and Clinical Use. *Cold Spring Harb Perspect Biol*. 2010;2:a001008–a. https://doi.org/10.1101/cshperspect.a001008.
6. Hassin O, Oren M. Drugging p53 in cancer: one protein, many targets. *Nat Rev Drug Discov*. 2023;22:127–144. https://doi.org/10.1038/s41573-022-00571-8.
7. Karni-Schmidt O, Lokshin M, Prives C. The Roles of MDM2 and MDMX in Cancer. *Annu Rev Pathol*. 2016;11:617–644. https://doi.org/10.1146/annurev-pathol-012414-040349.
8. Haupt Y, Maya R, Kazaz A, Oren M. Mdm2 promotes the rapid degradation of p53. *Nature*. 1997;387:296–299. https://doi.org/10.1038/387296a0.
9. Honda R, Tanaka H, Yasuda H. Oncoprotein MDM2 is a ubiquitin ligase E3 for tumor suppressor p53. *FEBS Lett*. 1997;420:25–27. https://doi.org/10.1016/S0014-5793(97)01480-4.
10. Migliorini D, Denchi EL, Danovi D, et al. Mdm4 (Mdmx) Regulates p53-Induced Growth Arrest and Neuronal Cell Death during Early Embryonic Mouse Development. *Mol Cell Biol*. 2002;22:5527–5538. https://doi.org/10.1128/MCB.22.15.5527-5538.2002.
11. Momand J, Zambetti GP, Olson DC, George D, Levine AJ. The mdm-2 oncogene product forms a complex with the p53 protein and inhibits p53-mediated transactivation. *Cell*. 1992;69:1237–1245. https://doi.org/10.1016/0092-8674(92)90644-R.
12. R. M. De Oca Luna, D. S. Wagner, G. Lozano, Rescue of early embryonic lethality in mdm2-deficient mice by deletion of p53, Nature 378 (1995) 203–206. DOI: 10.1038/378203a0.
13. Jones SN, Roe AE, Donehower LA, Bradley A. Rescue of embryonic lethality in Mdm2-deficient mice by absence of p53. *Nature*. 1995;378:206–208. https://doi.org/10.1038/378206a0.
14. Linke K, Mace PD, Smith CA, Vaux DL, Silke J, Day CL. Structure of the MDM2/MDMX RING domain heterodimer reveals dimerization is required for their ubiquitylation in trans. *Cell Death Differ*. 2008;15:841–848. https://doi.org/10.1038/sj.cdd.4402309.
15. Kawai H, Lopez-Pajares V, Kim MM, Wiederschain D, Yuan ZM. RING Domain-Mediated Interaction Is a Requirement for MDM2's E3 Ligase Activity. *Cancer Res*. 2007;67:6026–6030. https://doi.org/10.1158/0008-5472.CAN-07-1313.
16. Wu W, Xu C, Ling X, et al. Targeting RING domains of Mdm2-MdmX E3 complex activates apoptotic arm of the p53 pathway in leukemia/lymphoma cells. *Cell Death Dis*. 2015;6:e2035.
17. Kosztyu P, Slaninová I, Valčíková B, et al. A Single Conserved Amino Acid Residue as a Critical Context-Specific Determinant of the Differential Ability of Mdm2 and

MdmX RING Domains to Dimerize. *Front Physiol*. 2019;10:390. https://doi.org/10.3389/fphys.2019.00390.
18. Nomura K, Klejnot M, Kowalczyk D, et al. Structural analysis of MDM2 RING separates degradation from regulation of p53 transcription activity. *Nat Struct Mol Biol*. 2017;24:578–587. https://doi.org/10.1038/nsmb.3414.
19. Ilic VK, Egorova O, Tsang E, et al. Hinokiflavone Inhibits MDM2 Activity by Targeting the MDM2-MDMX RING Domain. *Biomolecules*. 2022;12:643. https://doi.org/10.3390/biom12050643.
20. Pellegrino M, Mancini F, Lucà R, et al. Targeting the MDM2/MDM4 Interaction Interface as a Promising Approach for p53 Reactivation Therapy. *Cancer Res*. 2015;75:4560–4572. https://doi.org/10.1158/0008-5472.CAN-15-0439.
21. Schrodinger Release 2019-4, Maestro, Schrödinger, LLC, New York, NY, 2019, (n.d.).
22. K. J. Bowers, F. D. Sacerdoti, J. K. Salmon, Y. Shan, D. E. Shaw, E. Chow, H. Xu, R. O. Dror, M. P. Eastwood, B. A. Gregersen, J. L. Klepeis, I. Kolossvary, M. A. Moraes, Scalable algorithms for molecular dynamics simulations on commodity clusters, in: Proc. 2006 ACMIEEE Conf. Supercomput. - SC 06, ACM Press, Tampa, Florida, 2006: p. 84. DOI: 10.1145/1188455.1188544.
23. Schrödinger Release 2019-4, Desmond Molecular Dynamics System, D. E. Shaw Research, New York, NY, 2019. Maestro-Desmond Interoperability Tools, Schrödinger, New York, NY, 2019, (n.d.).
24. Martyna GJ, Klein ML, Tuckerman M. Nosé-Hoover chains: The canonical ensemble via continuous dynamics. *J Chem Phys*. 1992;97:2635–2643. https://doi.org/10.1063/1.463940.
25. Martyna GJ, Tobias DJ, Klein ML. Constant pressure molecular dynamics algorithms. *J Chem Phys*. 1994;101:4177–4189. https://doi.org/10.1063/1.467468.
26. Tubert-Brohman I, Sherman W, Repasky M, Beuming T. Improved Docking of Polypeptides with Glide. *J Chem Inf Model*. 2013;53:1689–1699. https://doi.org/10.1021/ci400128m.
27. Manzor K, Kelleher F. Synthesis of orthogonally protected thioamide dipeptides for use in solid-phase peptide synthesis. *Tetrahedron Lett*. 2016;57:5237–5239. https://doi.org/10.1016/j.tetlet.2016.10.036.
28. van Herpt JT, Stuart MCA, Browne WR, Feringa BL. A Dithienylethene-Based Rewritable Hydrogelator. *Chem Eur J*. 2014;20:3077–3083. https://doi.org/10.1002/chem.201304064.
29. E. Gasteiger, C. Hoogland, A. Gattiker, S. Duvaud, M. R. Wilkins, R. D. Appel, A. Bairoch, Protein Identification and Analysis Tools on the Expasy Server, in: Proteomics Protoc. Handb., 1st ed., Humana Totowa, NJ, 2005: pp. 571–607.
30. M. Attili, M. Ballarotto, A. Gennari, A. Macchiarulo, F. Moretti, A. F. Saccoccia, Temperini, S. Valentini, Peptidi in grado di interferire con l'associazione dell'eterodimero MDM2/MDM4 e loro uso nel trattamento del cancro, IT102023000015816, 2023.
31. Duhr S, Braun D. Why molecules move along a temperature gradient. *Proc Natl Acad Sci*. 2006;103:19678–19682. https://doi.org/10.1073/pnas.0603873103.
32. Jerabek-Willemsen M, Wienken CJ, Braun D, Baaske P, Duhr S. Molecular Interaction Studies Using Microscale Thermophoresis. *Assay Drug Dev Technol*. 2011;9:342–353. https://doi.org/10.1089/adt.2011.0380.
33. Merlino F, Pecoraro A, Longobardi G, et al. Development and Nanoparticle-Mediated Delivery of Novel MDM2/MDM4 Heterodimer Peptide Inhibitors to Enhance 5-Fluorouracil Nucleolar Stress in Colorectal Cancer Cells. *J Med Chem*. 2024;67:1812–1824. https://doi.org/10.1021/acs.jmedchem.3c01312.